Hindawi Publishing Corporation
Advances in Condensed Matter Physics
Volume 2016, Article ID 5470429, 10 pages
http://dx.doi.org/10.1155/2016/5470429

Research Article

Theoretical Study of Upper Critical Magnetic Field (H_{C2}) in Multiband Iron Based Superconductors

Tsadik Kidanemariam[1] and Gebregziabher Kahsay[2]

[1]*Department of Physics, Adigrat University, P.O. Box 50, Adigrat, Ethiopia*
[2]*Department of Physics, College of Science, Bahir Dar University, P.O Box 79, Bahir Dar, Ethiopia*

Correspondence should be addressed to Tsadik Kidanemariam; tsadik.k@gmail.com

Received 23 August 2016; Revised 25 October 2016; Accepted 9 November 2016

Academic Editor: Prasenjit Guptasarma

This research work focuses on the theoretical investigation of the upper critical magnetic field, H_{C2}; Ginzburg-Landau coherence length, $\xi_{GL}(T)$; and Ginzburg-Landau penetration depth, $\lambda_{GL}(T)$, for the two-band iron based superconductors $BaFe_2(As_{1-x}P_x)_2$, $Nd(O_{1-x}F_x)FeAs$, and LiFeAs. By employing the phenomenological Ginzburg-Landau (GL) equation for the two-band superconductors $BaFe_2(As_{1-x}P_x)_2$, $Nd(O_{1-x}F_x)FeAs$, and LiFeAs, we obtained expressions for the upper critical magnetic field, H_{C2}; GL coherence length, ξ_{GL}; and GL penetration depth, λ_{GL}, as a function of temperature and the angular dependency of upper critical magnetic field. By using the experimental values in the obtained expressions, phase diagrams of the upper critical magnetic field parallel, $H_{C2}^{\parallel c}$, and perpendicular, $H_{C2}^{\perp c}$, to the symmetry axis (c-direction) versus temperature are plotted. We also plotted the phase diagrams of the upper critical magnetic field, H_{C2} versus the angle θ. Similarly, the phase diagrams of the GL coherence length, ξ_{GL}, and GL penetration depth, λ_{GL}, parallel and perpendicular to the symmetry axis versus temperature are drawn for the superconductors mentioned above. Our findings are in agreement with experimental observations.

1. Introduction

The discovery of superconductivity in iron based materials by Kamihara et al. [1] at $T_C = 26$ K in the iron-based superconductor $LaFeAsO_{1-x}F_x$ was a welcomed surprise and this brought to an end the monopoly of cuprates as the only high temperature superconductors. The T_C of F-doped LaOFeAs was reported to increase with pressure and reach a maximum of about 43 K at 4 GPa, obtained from electrical resistance measurements under high pressure [2]. Up to now, the critical temperature for iron based superconductors has been raised to 57.3 K for $Sm_{0.95}La_{0.05}O_{0.85}F_{0.15}FeAs$ which is the highest for noncuprate superconductors [3]. Among these new iron based superconductors, the iron based F-doped layered quaternary compound $Nd(O_{1-x}F_x)FeAs$ is a good candidate for this study since it is the same family as $LaFeAsO_{1-x}F_x$ and has the same crystal structure. Previous extensive transport and heat capacity studies on $Nd(O_{1-x}F_x)FeAs$ single crystal revealed that at zero external magnetic fields the compound was found to undergo a transition from the normal state to the superconducting state at superconducting critical temperature: $T_C = 51$ K at $x = 0.18$ at ambient pressure [4].

Superconductivity was also obtained in the 122-family iron based multiband superconductors and great efforts were made to raise T_C to temperatures higher than 38 K as detected in $(Ba_{0.6}K_{0.4})Fe_2As_2$ [5] and for optimally doped $BaFe_2(As_{1-x}P_x)_2$ at $T_C = 31$ K at $x = 0.32$ [6]. The isovalent doping of phosphorus for arsenic in $BaFe_2(As_{1-x}P_x)_2$ suppresses magnetic ordering without changing the number of Fe(3d) electrons and induces superconductivity with a maximum value of $T_C = 31$ K. The isovalently P-doped $BaFe_2(As_{1-x}P_x)_2$ system is particularly suitable to study the detailed evolution of the electronic properties. The isovalent doping does not add any charge carriers to the system and the dopant changes the electronic structure mainly because of differences in ion size.

The discovery of superconductivity in the 111-family of iron based superconductor, LiFeAs, is reported by Wang et al. [7]. The compound crystallizes into a structure containing [FeAs] conducting layer that is interlaced with Li charge

reservoir. Superconductivity was observed with T_C up to 18 K [7] in this compound. The two-band nature of the order parameter in LiFeAs is confirmed by heat capacity measurements [8] and by ab initio calculations [9]. Several methods have been used to determine the temperature dependence and anisotropy of H_{C2} for LiFeAs and the first results were obtained from resistivity measurements [10]. Among the iron based superconductors, LiFeAs shows a relatively small upper critical magnetic field.

Soon, after the discovery of superconductivity in iron based superconductors, it was found that the iron based superconductors possess a large superconducting critical magnetic field (H_{C2}) and low anisotropy [11] when compared to the cuprates. The theory of upper critical magnetic field in superconductors was essentially developed right after Abrikosov proposed the idea of type II superconductors [12]. Determining the upper critical magnetic field H_{C2}, where superconductivity ceases in a type II superconductor, is one of the most important steps for gathering and understanding of unconventional superconductivity including the pairing mechanism, the pairing strength, and the coherence length. In an anisotropic type II superconductors, the magnetic field destroys superconductivity at the upper critical magnetic fields H_{C2}^{ab} and H_{C2}^{c} when the magnetic field is applied within the *ab*-plane ($H \parallel ab$) and *c*-axis ($H \parallel c$), respectively. It is well known that the Ginzburg-Landau theory remains a powerful instrument for the study of magnetic phase diagram of superconductors [13]. The free energy functional of two-band superconductors can be expressed by the power series of order parameters in the vicinity of the critical temperature and minimization of the free energy function gives the GL equations that can describe the field distribution in superconductors.

In conventional superconductors, the electron pairing is mediated by an electron-phonon interaction and can be well understood within the microscopic-model developed by Bardeen, Cooper, and Schrieffer (BCS) in the theory of superconductivity [14]. The electron-phonon coupling mechanism is not sufficient to explain the superconductivity in iron based superconductors and their role is rather speculated by spin-fluctuation coupling mechanism.

The main specialty of iron based superconductors is their multiband nature. In the multiband model of superconductivity, several intraband and interband interaction terms are present. The importance of interband pairing in multiband models has been emphasized by de Menezes [15]. The Fermi surface, which has contributions from all five possible Fe(3d) orbitals [16], is very similar to the different iron based compounds and all the five Fe(3d) orbitals pass through the Fermi surface. The first-principle calculations have shown that the energy bands near the Fermi surface are mainly contributed by the Fe(3d) d_{xz} and d_{yz} orbitals [17]. One of the main features of two-band superconductors is the presence of two energy gaps, Δ_1 and Δ_2, which vanish at the same critical temperature, T_C. According to the microscopic theory, the presence of the two gaps is explained by the fact that in each band "*i*" an intraband coupling constant V_{ii} and the interband coupling constant V_{ij} exist which on the one hand enhances pairing of electrons and on the other hand leads to the single critical temperature, T_C.

2. Theoretical Formulations

2.1. Calculation of Upper Critical Magnetic Field. In the presence of two order parameters in a bulk isotropic s-wave superconductor, the phenomenological GL free energy density functional for two-band superconducting order parameters Ψ_1 and Ψ_2 can be written as [18]

$$F_{\mathrm{SC}} = F_1 + F_2 + F_{12} + \frac{H^2}{8\pi}, \tag{1}$$

where

$$\begin{aligned}
F_1 &= -\frac{\hbar^2}{2m_1^*}\left|\left(\nabla - \frac{2ie^*\mathbf{A}}{\hbar c}\right)\Psi_1\right|^2 - \alpha_1\left|\Psi_1\right|^2 + \frac{\beta_1}{2}\left|\Psi_1\right|^4,\\
F_2 &= -\frac{\hbar^2}{2m_2^*}\left|\left(\nabla - \frac{2ie^*\mathbf{A}}{\hbar c}\right)\Psi_2\right|^2 - \alpha_2\left|\Psi_2\right|^2 + \frac{\beta_2}{2}\left|\Psi_2\right|^4,\\
F_{12} &= \epsilon\left(\Psi_1\Psi_2^* + \Psi_2\Psi_1^*\right)\\
&\quad + \epsilon_1\left(\left[\left(\nabla + \frac{2ie^*\mathbf{A}}{\hbar c}\right)^*\Psi_1^*\left(\nabla - \frac{2ie^*\mathbf{A}}{\hbar c}\right)\Psi_2\right]\right.\\
&\quad \left. + \left[\left(\nabla + \frac{2ie^*\mathbf{A}}{\hbar c}\right)^*\Psi_2^*\left(\nabla - \frac{2ie^*\mathbf{A}}{\hbar c}\right)\Psi_1\right]\right),
\end{aligned} \tag{2}$$

where F_1 and F_2 are the free energies for each band. F_{12} is the interaction free energy term between the two bands. $H^2/8\pi$ is the energy stored in the local magnetic fields. Ψ_1 and Ψ_2 are superconducting order parameters. The coefficients ϵ and ϵ_1 describe the interband interaction of the two order parameters (proximity effect) and the interband mixing of gradients of two order parameters (drag effect) [18], respectively. m_1^* and m_2^* denote the effective mass of carriers for each band. α is the GL temperature-dependent parameter and β_i is GL temperature-independent parameter. $\mathbf{H} = \nabla \times \mathbf{A}$ is the external magnetic field and $\mathbf{A}$ is the vector potential.

Now, substituting (2) into (1), we get

$$\begin{aligned}
F_{\mathrm{SC}} &= -\frac{\hbar^2}{2m_1^*}\left|\left(\nabla - \frac{2ie^*\mathbf{A}}{\hbar c}\right)\Psi_1\right|^2 - \alpha_1\left|\Psi_1\right|^2 + \frac{\beta_1}{2}\left|\Psi_1\right|^4\\
&\quad - \frac{\hbar^2}{2m_2^*}\left|\left(\nabla - \frac{2ie^*\mathbf{A}}{\hbar c}\right)\Psi_2\right|^2 - \alpha_2\left|\Psi_2\right|^2 + \frac{\beta_2}{2}\left|\Psi_2\right|^4\\
&\quad + \epsilon\left(\Psi_1\Psi_2^* + \Psi_2\Psi_1^*\right)\\
&\quad + \epsilon_1\left(\left[\left(\nabla + \frac{2ie^*\mathbf{A}}{\hbar c}\right)^*\Psi_1^*\left(\nabla - \frac{2ie^*\mathbf{A}}{\hbar c}\right)\Psi_2\right]\right.\\
&\quad \left. + \left[\left(\nabla + \frac{2ie^*\mathbf{A}}{\hbar c}\right)^*\Psi_2^*\left(\nabla - \frac{2ie^*\mathbf{A}}{\hbar c}\right)\Psi_1\right]\right) + \frac{H^2}{8\pi}.
\end{aligned} \tag{3}$$

In order to derive the GL equations for the two-gap superconductor, we minimize the free energy function given in (3) with

respect to variations in the complex conjugate of the order parameters Ψ_1^*, Ψ_2^*, such that

$$\frac{\partial F_{SC}}{\partial \Psi_1^*} = 0, \qquad \frac{\partial F_{SC}}{\partial \Psi_2^*} = 0. \tag{4}$$

Near the critical temperature, T_C, we have $\Psi_{1,2}^3 \to 0$. Thus, using (3) in (4), the first GL equations for the two bands can be obtained as

$$-\frac{\hbar^2}{2m_1^*}\left(\nabla - \frac{2ie^*\mathbf{A}}{\hbar c}\right)^2 \Psi_1 - \alpha_1\Psi_1 + \epsilon\Psi_2 + \epsilon_1\left(\nabla - \frac{2ie^*\mathbf{A}}{\hbar c}\right)^2 \Psi_2 = 0,$$
$$-\frac{\hbar^2}{2m_2^*}\left(\nabla - \frac{2ie^*\mathbf{A}}{\hbar c}\right)^2 \Psi_2 - \alpha_2\Psi_2 + \epsilon\Psi_1 + \epsilon_1\left(\nabla - \frac{2ie^*\mathbf{A}}{\hbar c}\right)^2 \Psi_1 = 0. \tag{5}$$

Equation (5) can be expressed in terms of matrix product form as

$$\begin{pmatrix} H_{11} & H_{12} \\ H_{21} & H_{22} \end{pmatrix}\begin{pmatrix} \Psi_1 \\ \Psi_2 \end{pmatrix} = \begin{pmatrix} -\frac{\hbar^2}{2m_1^*}\left(\nabla - \frac{2ie^*\mathbf{A}}{\hbar c}\right)^2 - \alpha_1 & \epsilon + \epsilon_1\left(\nabla - \frac{2ie^*\mathbf{A}}{\hbar c}\right)^2 \\ \epsilon + \epsilon_1\left(\nabla - \frac{2ie^*\mathbf{A}}{\hbar c}\right)^2 & -\frac{\hbar^2}{2m_2^*}\left(\nabla - \frac{2ie^*\mathbf{A}}{\hbar c}\right)^2 - \alpha_2 \end{pmatrix}\begin{pmatrix} \Psi_1 \\ \Psi_2 \end{pmatrix} = 0. \tag{6}$$

We can compare (6) to the free-particle time independent Schrödinger equation with particle of mass m_i and charge of e^* moving in a magnetic field which is the same as eigenvalues of the harmonic oscillator. For the field in the direction of the c-axis, we can linearize the GL equations as follows:

$$H_{11}\Psi_1 = -\frac{\hbar^2}{2m_1^*}\left(\nabla - \frac{2ie^*\mathbf{A}}{\hbar c}\right)^2 \Psi_1 = E_{11}\Psi_1,$$
$$H_{22}\Psi_2 = -\frac{\hbar^2}{2m_2^*}\left(\nabla - \frac{2ie^*\mathbf{A}}{\hbar c}\right)^2 \Psi_2 = E_{22}\Psi_2. \tag{7}$$

Hence, (6) becomes

$$\begin{pmatrix} E_{11} - \alpha_1 & \epsilon + \epsilon_1\left(\nabla - \frac{2ie^*\mathbf{A}}{\hbar c}\right)^2 \\ \epsilon + \epsilon_1\left(\nabla - \frac{2ie^*\mathbf{A}}{\hbar c}\right)^2 & E_{22} - \alpha_2 \end{pmatrix}\begin{pmatrix} \Psi_1 \\ \Psi_2 \end{pmatrix} = 0. \tag{8}$$

The energy eigenvalues of the quantum harmonic oscillator are given by $E_n = (n + 1/2)\hbar\omega_i$. In order to determine H_{C2}, we must choose $n = 0$ which gives the upper critical magnetic field. The energy of the two bands for the $n = 0$ state becomes $E_{11} = (1/2)\hbar\omega_1$ and $E_{22} = (1/2)\hbar\omega_2$ where the frequency of the oscillator is given by $\omega_i = 2e^*H_{C2}/m_i^*c$. For a displacement x in one direction, the vector potential is given by $\mathbf{A} = H_{C2}x$.

Thus, (8) can be written as

$$\begin{pmatrix} \frac{\hbar e^* H_{C2}}{m_1^* c} - \alpha_1 & \epsilon - \epsilon_1\frac{2e^*H_{C2}}{\hbar c} \\ \epsilon - \epsilon_1\frac{2e^*H_{C2}}{\hbar c} & \frac{\hbar e^* H_{C2}}{m_2^* c} - \alpha_2 \end{pmatrix}\begin{pmatrix} \Psi_1 \\ \Psi_2 \end{pmatrix} = 0. \tag{9}$$

By considering $m_1^* = m_2^* = m^*$, the upper critical magnetic field H_{C2} is obtained by setting the determinant of the matrix in (9) to zero; that is,

$$\begin{vmatrix} \frac{\hbar e^* H_{C2}}{m^* c} - \alpha_1 & \epsilon - \epsilon_1\frac{2e^*H_{C2}}{\hbar c} \\ \epsilon - \epsilon_1\frac{2e^*H_{C2}}{\hbar c} & \frac{\hbar e^* H_{C2}}{m^* c} - \alpha_2 \end{vmatrix} = 0, \tag{10}$$

from which we get

$$\left[\left(\frac{e^*\hbar}{m^*c}\right)^2 - \frac{4e^{*2}\epsilon_1^2}{\hbar^2c^2}\right]H_{C2}^2 - \left[\frac{e^*\hbar}{m^*c}(\alpha_1+\alpha_2) - \frac{4e^*\epsilon\epsilon_1}{\hbar c}\right]H_{C2} + \alpha_1\alpha_2 - \epsilon^2 = 0. \tag{11}$$

Finally, the solution of the quadratic equation becomes

$$H_{C2} = \frac{(e^*\hbar/m^*c)(\alpha_1+\alpha_2) - 4e^*\epsilon\epsilon_1/\hbar c \pm \sqrt{(e^{*2}\hbar^2/m^{*2}c^2)[\alpha_1^2+\alpha_2^2] - (2e^{*2}\hbar^2/m^{*2}c^2)\alpha_1\alpha_2 - (8e^{*2}\epsilon\epsilon_1/m^*c^2)[\alpha_1+\alpha_2] + (16e^{*2}\epsilon_1^2/\hbar^2c^2)\alpha_1\alpha_2 + 4e^{*2}\hbar^2\epsilon^2/m^{*2}c^2}}{2\left[(e^*\hbar/m^*c)^2 - 4e^{*2}\epsilon_1^2/\hbar^2c^2\right]}. \tag{12}$$

Now let $\alpha_1 = \hbar^2/2m^*\xi_{GL1}^2$, $\alpha_2 = \hbar^2/2m^*\xi_{GL2}^2$, and $\epsilon = \hbar^2/2m^*\xi_{GL12}^2$, where ξ_{GL1}, ξ_{GL2}, and ξ_{GL12} are the first band, second band, and interband effective coherence lengths, respectively, $\epsilon_1 = \upsilon\hbar^2/2m^*$, where υ is the gradients of interband mixing of two order parameters in energy unit and $\Phi_0 = 2\pi\hbar/e^*$ and is the quantum flux.

Hence, (12) becomes

$$H_{C2} = \frac{\Phi_0}{2\pi\left(1-\upsilon^2\right)}\left(\frac{1}{2\xi_{GL1}^2}+\frac{1}{2\xi_{GL2}^2}-\frac{\upsilon}{\xi_{GL12}^2}\right) \pm \frac{\Phi_0}{2\pi\left(1-\upsilon^2\right)}\left[\left(\frac{1}{2\xi_{GL1}^2}+\frac{1}{2\xi_{GL2}^2}-\frac{\upsilon}{\xi_{GL12}^2}\right)^2 - \left(1-\upsilon^2\right)\left(\frac{1}{\xi_{GL1}^2\xi_{GL2}^2}-\frac{1}{\xi_{GL12}^4}\right)\right]^{1/2}. \tag{13}$$

Now, let us consider cases as follows.

Case 1. Consider

$$\left(\frac{1}{2\xi_{GL1}^2}+\frac{1}{2\xi_{GL2}^2}-\frac{\upsilon}{\xi_{GL12}^2}\right)^2 \ll \left(1-\upsilon^2\right)\left(\frac{1}{\xi_{GL1}^2\xi_{GL2}^2}-\frac{1}{\xi_{GL12}^4}\right), \tag{14}$$

In this case the term in the square root in (13) becomes complex. Therefore, we can conclude that the first case is not valid since magnetic field is a real quantity.

Case 2. Consider

$$\left(\frac{1}{2\xi_{GL1}^2}+\frac{1}{2\xi_{GL2}^2}-\frac{\upsilon}{\xi_{GL12}^2}\right)^2 \gg \left(1-\upsilon^2\right)\left(\frac{1}{\xi_{GL1}^2\xi_{GL2}^2}-\frac{1}{\xi_{GL12}^4}\right). \tag{15}$$

Using Taylor's binomial series expansions, for the negative value of the term in the square root in (13) we get

$$H_{C2}^- = \frac{\Phi_0}{2\pi}\frac{1}{2}\frac{\left(1/\xi_{GL1}^2\xi_{GL2}^2-1/\xi_{GL12}^4\right)}{\left(1/2\xi_{GL1}^2+1/2\xi_{GL2}^2-\upsilon/\xi_{GL12}^2\right)} - \frac{1}{8}\frac{\Phi_0}{2\pi}\left(\frac{\left(1-\upsilon^2\right)\left(1/\xi_{GL1}^2\xi_{GL2}^2-1/\xi_{GL12}^4\right)^2}{\left(1/2\xi_{GL1}^2+1/2\xi_{GL2}^2-\upsilon/\xi_{GL12}^2\right)^3}\right). \tag{16}$$

For the positive value of the square root in (13) we get

$$H_{C2}^+ = \frac{\Phi_0}{2\pi\left(1-\upsilon^2\right)}\left(\frac{1}{2\xi_{GL1}^2}+\frac{1}{2\xi_{GL2}^2}-\frac{\upsilon}{\xi_{GL12}^2}\right) - \frac{\Phi_0}{2\pi}\frac{1}{2}\frac{\left(1/\xi_{GL1}^2\xi_{GL2}^2-1/\xi_{GL12}^4\right)}{\left(1/2\xi_{GL1}^2+1/2\xi_{GL2}^2-\upsilon/\xi_{GL12}^2\right)} + \frac{1}{8}\frac{\Phi_0}{2\pi}\left(\frac{\left(1-\upsilon^2\right)\left(1/\xi_{GL1}^2\xi_{GL2}^2-1/\xi_{GL12}^4\right)^2}{\left(1/2\xi_{GL1}^2+1/2\xi_{GL2}^2-\upsilon/\xi_{GL12}^2\right)^3}\right). \tag{17}$$

Due to the drag effect, the GL theory for a two-band superconductor can be reduced to the GL theory for an effective single-band superconductor. Two-band model can be reduced to one band model if we set $\alpha_2 = \epsilon = \epsilon_1 = 0$. We observe that (16) cannot be reduced to one band model. So it does not have a physical meaning. But (17) can be reduced to one band model and is the analytical equation of upper critical magnetic field and thus we have

$$H_{C2} = \frac{\Phi_0}{2\pi\xi_{GL12}^2}\left(\frac{\xi_{GL12}^2}{\xi_{GL1}^2}+\frac{\xi_{GL12}^2}{\xi_{GL2}^2}-2\upsilon\right)\left[\frac{1}{1-\upsilon^2} - \frac{\xi_{GL12}^2/\xi_{GL1}^2\xi_{GL2}^2-1}{\left(\xi_{GL12}^2/\xi_{GL1}^2+\xi_{GL12}^2/\xi_{GL2}^2-2\upsilon\right)^2} + \frac{\left(1-\upsilon^2\right)\left(\xi_{GL12}^4/\xi_{GL1}^2\xi_{GL2}^2-1\right)^2}{\left(\xi_{GL12}^2/\xi_{GL1}^2+\xi_{GL12}^2/\xi_{GL2}^2-2\upsilon\right)^4}\right]. \tag{18}$$

The effect of anisotropy mass tensor on the upper critical magnetic field is included by replacing ξ in (18) with coherence length tensor, $\boldsymbol{\xi}$.

Finally we have

$$H_{C2} = \frac{\Phi_0}{2\pi\boldsymbol{\xi}_{GL12}^2\sqrt{\sin^2\theta+\gamma^2\cos^2\theta}}\left(\frac{\boldsymbol{\xi}_{GL12}^2}{\boldsymbol{\xi}_{GL1}^2}+\frac{\boldsymbol{\xi}_{GL12}^2}{\boldsymbol{\xi}_{GL2}^2}-2\upsilon\right)\left[\frac{1}{1-\upsilon^2} - \frac{\boldsymbol{\xi}_{GL12}^2/\boldsymbol{\xi}_{GL1}^2\boldsymbol{\xi}_{GL2}^2-1}{\left(\boldsymbol{\xi}_{GL12}^2/\boldsymbol{\xi}_{GL1}^2+\boldsymbol{\xi}_{GL12}^2/\boldsymbol{\xi}_{GL2}^2-2\upsilon\right)^2} + \frac{\left(1-\upsilon^2\right)\left(\boldsymbol{\xi}_{GL12}^4/\boldsymbol{\xi}_{GL1}^2\boldsymbol{\xi}_{GL2}^2-1\right)^2}{\left(\boldsymbol{\xi}_{GL12}^2/\boldsymbol{\xi}_{GL1}^2+\boldsymbol{\xi}_{GL12}^2/\boldsymbol{\xi}_{GL2}^2-2\upsilon\right)^4}\right]. \tag{19}$$

The interband mixing of gradients of two order parameters in an isotropic bulk two-band superconductor plays important role. The two-band superconductor is characterized with a single upper critical magnetic field, H_{C2}; GL coherence length, ξ_{GL}; GL penetration depth, λ_{GL}; and GL characteristic parameter, κ.

Thus, the GL effective coherence length, ξ_{GLeff}, can be expressed as

$$\frac{1}{\xi^2_{\mathrm{GLeff}}} = \frac{1}{\xi^2_{\mathrm{GL12}}}\left(\frac{\xi^2_{\mathrm{GL12}}}{\xi^2_{\mathrm{GL1}}} + \frac{\xi^2_{\mathrm{GL12}}}{\xi^2_{\mathrm{GL2}}} - 2v\right)\left[\frac{1}{1-v^2}\right. - \frac{\xi^2_{\mathrm{GL12}}/\xi^2_{\mathrm{GL1}}\xi^2_{\mathrm{GL2}} - 1}{\left(\xi^2_{\mathrm{GL12}}/\xi^2_{\mathrm{GL1}} + \xi^2_{\mathrm{GL12}}/\xi^2_{\mathrm{GL2}} - 2v\right)^2} + \left.\frac{\left(1-v^2\right)\left(\xi^4_{\mathrm{GL12}}/\xi^2_{\mathrm{GL1}}\xi^2_{\mathrm{GL2}} - 1\right)^2}{\left(\xi^2_{\mathrm{GL12}}/\xi^2_{\mathrm{GL1}} + \xi^2_{\mathrm{GL12}}/\xi^2_{\mathrm{GL2}} - 2v\right)^4}\right]. \tag{20}$$

Therefore, (19) becomes

$$H_{C2}(T) = \frac{\Phi_0}{2\pi\xi^2_{\mathrm{GLeff}}(T)\sqrt{\sin^2\theta + \gamma^2\cos^2\theta}}. \tag{21}$$

If the direction of the applied magnetic field is parallel to the c-axis, then the expression for the upper critical magnetic field, $H^{\|c}_{C2}$, as function of temperature in (21) is given by

$$H^{\|c}_{C2}(T) = \frac{\Phi_0}{2\pi\left(\xi^{ab}_{\mathrm{GL}}\right)^2(0)}\left[1 - \left(\frac{T}{T_C}\right)^2\right], \tag{22}$$

where $H^{\|c}_{C2}(0) = \Phi_0/2\pi(\xi^{ab}_{\mathrm{GL}})^2(0)$ is the zero temperature upper critical field parallel to the c-axis.

If the direction of the applied magnetic field is perpendicular to the c-axis, then the expression for the upper critical magnetic field, $H^{\perp c}_{c2}(T)$, in (21) is given by

$$H^{\perp c}_{C2}(T) = \frac{\Phi_0}{2\pi\xi^{ab}_{\mathrm{GL}}(0)\,\xi^{c}_{\mathrm{GL}}(0)}\left[1 - \left(\frac{T}{T_C}\right)^2\right], \tag{23}$$

where $H^{\perp c}_{C2}(0) = \Phi_0/2\pi\xi^{ab}_{\mathrm{GL}}(0)\xi^{c}_{\mathrm{GL}}(0)$ is the zero temperature upper critical field perpendicular to the c-axis.

Using the experimental values $H^{\|c}_{C2}(0) = 36$ T and $H^{\perp c}_{C2}(0) = 77$ T [19] at $T_C = 31$ K, the mathematical expressions of the temperature dependence of the upper critical magnetic field parallel to the symmetry axis (in the c-direction) $H^{\|c}_{C2}(T)$ and perpendicular to the symmetry axis $H^{\perp c}_{C2}(T)$ in $BaFe_2(As_{1-x}P_x)_2$ become

$$H^{\|c}_{C2}(T) = 36\ \mathrm{Tesla}\left[1 - \left(\frac{T}{T_C}\right)^2\right], \qquad H^{\perp c}_{C2}(T) = 77\ \mathrm{Tesla}\left[1 - \left(\frac{T}{T_C}\right)^2\right]. \tag{24}$$

Ginzburg-Landau (GL) theory [20] can be used to determine the effect of an anisotropic effective mass m^* on the angular dependence as

$$\left(\frac{H^{\mathrm{GL}}_{C2}(\theta)\sin\theta}{H^{\perp c}_{C2}}\right)^2 + \left(\frac{H^{\mathrm{GL}}_{C2}(\theta)\cos\theta}{H^{\|c}_{C2}}\right)^2 = 1. \tag{25}$$

Finally, the angular dependence of the upper critical magnetic field for $BaFe_2(As_{1-x}P_x)_2$ at an angle θ from the c-axis can be expressed as

$$H^{\mathrm{GL}}_{C2}(\theta) = \frac{H^{\|c}_{C2}}{\sqrt{\cos^2\theta + \gamma^{-2}\sin^2\theta}}, \tag{26}$$

$$\mathrm{H}^{\mathrm{GL}}_{C2}(\theta) = \frac{36}{\sqrt{\cos^2\theta + 0.2186\sin^2\theta}}. \tag{27}$$

It has been shown that a single band anisotropic model can properly describe the angular dependence of $H_{C2}(\theta)$ in a multiband system near T_C [21].

Similarly, the current model/theory can be applied to 1111-family of iron based two-band superconductor $Nd(O_{1-x}F_x)FeAs$ by considering its experimental values. The expressions of the temperature dependence of the upper critical magnetic field parallel and perpendicular to the symmetry axis (in the c-axis) in $Nd(O_{1-x}F_x)FeAs$ for $H^{\|c}_{C2}(0) = 70$ T and $H^{\perp c}_{C2}(0) = 304$ T [7] at $T_C = 51$ K become

$$H^{\|c}_{C2}(T) = 70\ \mathrm{Tesla}\left[1 - \left(\frac{T}{T_C}\right)^2\right], \qquad H^{\perp c}_{C2}(T) = 304\ \mathrm{Tesla}\left[1 - \left(\frac{T}{T_C}\right)^2\right]. \tag{28}$$

The angular dependence of the upper critical magnetic field at an angle θ from the c-axis can be expressed as

$$H^{\mathrm{GL}}_{C2}(\theta) = \frac{70}{\sqrt{\cos^2\theta + 0.053\sin^2\theta}}. \tag{29}$$

Furthermore, the model/theory can be applied to the 111-family of iron based superconductor LiFeAs by considering its experimental values. The expressions of the temperature dependence of the upper critical magnetic field parallel and perpendicular to the symmetry axis (in the c-axis) in LiFeAs for $H^{\|c}_{C2}(0) = 15$ T and $H^{\perp c}_{C2}(0) = 24.2$ T [22] at $T_C = 18$ K become

$$H^{\|c}_{C2}(T) = 15\ \mathrm{Tesla}\left[1 - \left(\frac{T}{T_C}\right)^2\right], \qquad H^{\perp c}_{C2}(T) = 24.2\ \mathrm{Tesla}\left[1 - \left(\frac{T}{T_C}\right)^2\right]. \tag{30}$$

The angular dependence of the upper critical magnetic field at an angle θ from the c-axis can be expressed as

$$H^{\mathrm{GL}}_{C2}(\theta) = \frac{15}{\sqrt{\cos^2\theta + 0.38\sin^2\theta}}. \tag{31}$$

The expression for the anisotropy parameter (γ) is given by $\gamma = H^{\perp c}_{C2}/H^{\|c}_{C2}$. Thus, we calculate the values of γ to be 2.14, 4.34, and 1.6 for $BaFe_2(As_{1-x}P_x)_2$, $Nd(O_{1-x}F_x)FeAs$, and LiFeAs, respectively.

2.2. Calculation of Ginzburg-Landau Coherence Length and Penetration Depth. There are two important temperature dependent material parameters which arise from the GL model that characterize the phenomenological properties of a superconductor. The coherence length, ξ_{GL}, is defined as

$$\xi_{GL}(T) = \left(\frac{\hbar^2}{2m^* |\alpha(T)|}\right)^{1/2}. \quad (32)$$

This parameter specifies the spatial width of the transition layer of the order parameter, Ψ, in the neighborhood of the boundary between a normal region and a superconducting region.

Using the assumption of Changjan and Udomsamuthirun [23], the GL temperature-dependent parameter, α, can be written as a function of temperature in the vicinity of the critical temperature, T_C, as

$$\alpha_i(T) \approx \alpha_0 \left[1 - \left(\frac{T}{T_C}\right)^2\right]. \quad (33)$$

Here, α_0 is the temperature-independent positive constant.

Hence, the expression for the temperature dependent GL coherence length, $\xi_{GL}(T)$, becomes

$$\xi_{GL}(T) = \xi_{GL}(0)\left[1 - \left(\frac{T}{T_C}\right)^2\right]^{-1/2}, \quad (34)$$

where $\xi_{GL}(0)$ is the zero temperature coherence length. Using the experimental values of the zero temperature coherence lengths $\xi^{ab}_{GL}(0) = 3.2\,\text{nm}$ and $\xi^{c}_{GL}(0) = 1.3\,\text{nm}$ [19], the temperature dependent coherence length in the *ab*-plane, ξ^{ab}_{GL}, and along the *c*-axis, ξ^{c}_{GL}, for $BaFe_2(As_{1-x}P_x)_2$ becomes

$$\xi^{ab}_{GL}(T) = 3.2\,\text{nm}\left[1 - \left(\frac{T}{T_C}\right)^2\right]^{-1/2}, \quad (35)$$

$$\xi^{c}_{GL}(T) = 1.3\,\text{nm}\left[1 - \left(\frac{T}{T_C}\right)^2\right]^{-1/2}. \quad (36)$$

Similarly, using the experimental values of the zero temperature coherence lengths $\xi^{ab}_{GL}(0) = 3.7\,\text{nm}$ and $\xi^{c}_{GL}(0) = 0.9\,\text{nm}$ [24], the temperature dependent coherence length in the *ab*-plane, ξ^{ab}_{GL}, and along the *c*-axis, ξ^{c}_{GL}, for $Nd(O_{1-x}F_x)FeAs$ becomes

$$\xi^{ab}_{GL}(T) = 3.7\,\text{nm}\left[1 - \left(\frac{T}{T_C}\right)^2\right]^{-1/2}, \quad (37)$$

$$\xi^{c}_{GL}(T) = 0.9\,\text{nm}\left[1 - \left(\frac{T}{T_C}\right)^2\right]^{-1/2}. \quad (38)$$

Furthermore, using the experimental values of the zero temperature coherence lengths $\xi^{ab}_{GL}(0) = 4.8\,\text{nm}$ and $\xi^{c}_{GL}(0) = 1.7\,\text{nm}$ [22], the temperature dependent coherence length in the *ab*-plane, ξ^{ab}_{GL}, and along the *c*-axis, ξ^{c}_{GL}, for LiFeAs becomes

$$\xi^{ab}_{GL}(T) = 4.8\,\text{nm}\left[1 - \left(\frac{T}{T_C}\right)^2\right]^{-1/2}, \quad (39)$$

$$\xi^{c}_{GL}(T) = 1.7\,\text{nm}\left[1 - \left(\frac{T}{T_C}\right)^2\right]^{-1/2}. \quad (40)$$

According to the Meissner effect, an external magnetic field is expelled completely from the interior of a superconductor. But there was experimental evidence that magnetic fields penetrate a superconductor and a surface current flows in a very thin layer of thickness which is called the GL penetration depth, λ_{GL}, and can be expressed in terms of the superconducting electron density, n_s, as

$$\lambda_{GL}(T) = \left(\frac{m^* c^2}{16\pi e^{*2} n_s}\right)^{1/2}. \quad (41)$$

For $T \to 0$, $n_s \to n$ (total electron density), thus, we have

$$\lambda_{GL}(0) = \left(\frac{m^* c^2}{16\pi e^{*2} n}\right)^{1/2}. \quad (42)$$

In the two-fluid theory of Gorter and Casimir [25] we can have

$$\frac{n_s}{n} = \left[1 - \left(\frac{T}{T_C}\right)^4\right]. \quad (43)$$

Now, combining (41), (42), and (43) we have

$$\lambda_{GL}(T) = \lambda_{GL}(0)\left[1 - \left(\frac{T}{T_C}\right)^4\right]^{-1/2}. \quad (44)$$

Using the experimental value $\lambda^{ab}_{GL}(0) = 101\,\text{nm}$ [26] for $BaFe_2(As_{1-x}P_x)_2$, the expressions for the temperature dependent penetration depth in the *ab*-plane, λ^{ab}_{GL}, and along the *c*-axis, λ^{c}_{GL}, become

$$\lambda^{ab}_{GL}(T) = 101\,\text{nm}\left[1 - \left(\frac{T}{T_C}\right)^4\right]^{-1/2},$$
$$\lambda^{c}_{GL}(T) = 216\,\text{nm}\left[1 - \left(\frac{T}{T_C}\right)^4\right]^{-1/2}. \quad (45)$$

Similarly, using the experimental value $\lambda^{ab}_{GL}(0) = 200\,\text{nm}$ [24], the expressions for the temperature dependent penetration depth in the *ab*-plane, λ^{ab}_{GL}, and along the *c*-axis, λ^{c}_{GL}, for $Nd(O_{1-x}F_x)FeAs$ become

$$\lambda^{ab}_{GL}(T) = 200\,\text{nm}\left[1 - \left(\frac{T}{T_C}\right)^4\right]^{-1/2},$$
$$\lambda^{c}_{GL}(T) = 868.6\,\text{nm}\left[1 - \left(\frac{T}{T_C}\right)^4\right]^{-1/2}. \quad (46)$$

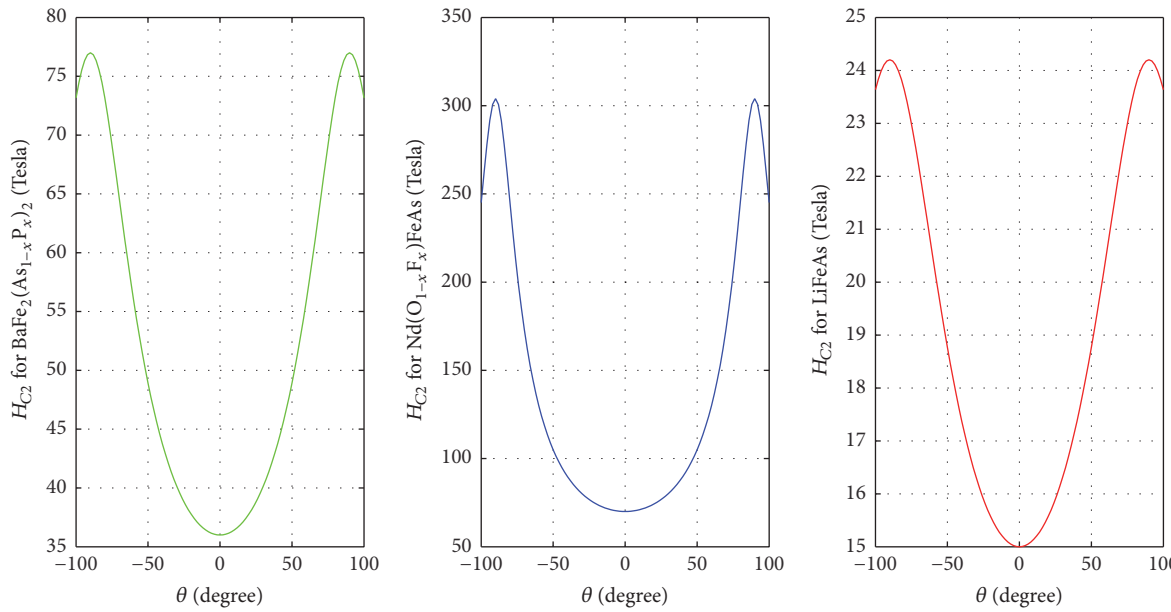

FIGURE 1: Variation of upper critical magnetic field H_{C2} with the angle θ for $BaFe_2(As_{1-x}P_x)_2$, $Nd(O_{1-x}F_x)FeAs$, and LiFeAs.

Using the experimental values $\lambda^{ab}_{GL}(0) = 198.4\,\text{nm}$ and $\lambda^{c}_{GL}(0) = 250\,\text{nm}$ [27], the expressions for the temperature dependent penetration depth in the ab-plane, λ^{ab}_{GL}, and along the c-axis, λ^{c}_{GL}, for LiFeAs become

$$\lambda^{ab}_{GL}(T) = 198.4\,\text{nm}\left[1-\left(\frac{T}{T_C}\right)^4\right]^{-1/2},$$
$$\lambda^{c}_{GL}(T) = 250\,\text{nm}\left[1-\left(\frac{T}{T_C}\right)^4\right]^{-1/2}. \quad (47)$$

The GL parameters in the c-axis and ab-plane are given by $\kappa^{c}_{GL} = \boldsymbol{\lambda}^{ab}_{GL}/\boldsymbol{\xi}^{ab}_{GL}$ and $\kappa^{ab}_{GL} = \sqrt{\boldsymbol{\lambda}^{ab}_{GL}\boldsymbol{\lambda}^{c}_{GL}/\boldsymbol{\xi}^{ab}_{GL}\boldsymbol{\xi}^{c}_{GL}}$, respectively [28].

Using the experimental values at $T = 0\,\text{K}$ for $BaFe_2(As_{1-x}P_x)_2$, κ_{GL} becomes

$$\kappa^{c}_{GL} = 31.6,$$
$$\kappa^{ab}_{GL} = 72.4. \quad (48)$$

Using the experimental values at $T = 0\,\text{K}$ for $Nd(O_{1-x}F_x)FeAs$, κ_{GL} becomes

$$\kappa^{c}_{GL} = 54,$$
$$\kappa^{ab}_{GL} = 228.4. \quad (49)$$

Similarly, at $T = 0\,\text{K}$ for LiFeAs, κ_{GL} becomes

$$\kappa^{c}_{GL} = 41.3,$$
$$\kappa^{ab}_{GL} = 78. \quad (50)$$

As is well known, Abrikosov showed that the breakdown point between type I and type II superconductors is $\kappa = 1/\sqrt{2}$ [12]. If the value of $\kappa < 1/\sqrt{2}$, then the superconductor is said to be type I and is type II if $\kappa > 1/\sqrt{2}$. Therefore, from (48) to (50), we conclude that the iron based superconductors $BaFe_2(As_{1-x}P_x)_2$, $Nd(O_{1-x}F_x)FeAs$, and LiFeAs are type II superconductors.

3. Results and Discussion

In this study we obtained expressions for the angular dependence of upper critical magnetic field, temperature dependence of the upper critical magnetic field parallel and perpendicular to the symmetry axis, the temperature dependence of ξ_{GL} and λ_{GL} parallel and perpendicular to the symmetry axis by using the GL approach in two-band iron based superconductors $BaFe_2(As_{1-x}P_x)_2$, $Nd(O_{1-x}F_x)FeAs$, and LiFeAs.

Firstly, using (27), (29), and (31) the phase diagram of H_{C2} versus θ is plotted for iron based superconductors $BaFe_2(As_{1-x}P_x)_2$, $Nd(O_{1-x}F_x)FeAs$, and LiFeAs, respectively, as shown in Figure 1. As can be seen from Figure 1, the upper critical magnetic field is maximum in the ab-plane ($\pm 90^\circ$) and minimum in the c-axis (0°) for $BaFe_2(As_{1-x}P_x)_2$, $Nd(O_{1-x}F_x)FeAs$, and LiFeAs.

Secondly, using (24), (28), and (30) and by taking some available experimental data, the phase diagrams of $H^{\parallel c}_{C2}$ and $H^{\perp c}_{C2}$ versus temperature are plotted for $BaFe_2(As_{1-x}P_x)_2$, $Nd(O_{1-x}F_x)FeAs$, and LiFeAs, respectively, as shown in Figure 2. As can be seen from Figure 2, the upper critical magnetic field decreases with increasing temperature and has nonlinear dependence for $BaFe_2(As_{1-x}P_x)_2$, $Nd(O_{1-x}F_x)FeAs$, and LiFeAs.

Thirdly, the expressions for the temperature dependent ξ^{ab}_{GL} and ξ^{c}_{GL} for $BaFe_2(As_{1-x}P_x)_2$, $Nd(O_{1-x}F_x)FeAs$, and LiFeAs are given in (35) and (36); (37) and (38); (39) and (40), respectively. Using those equations and by considering some

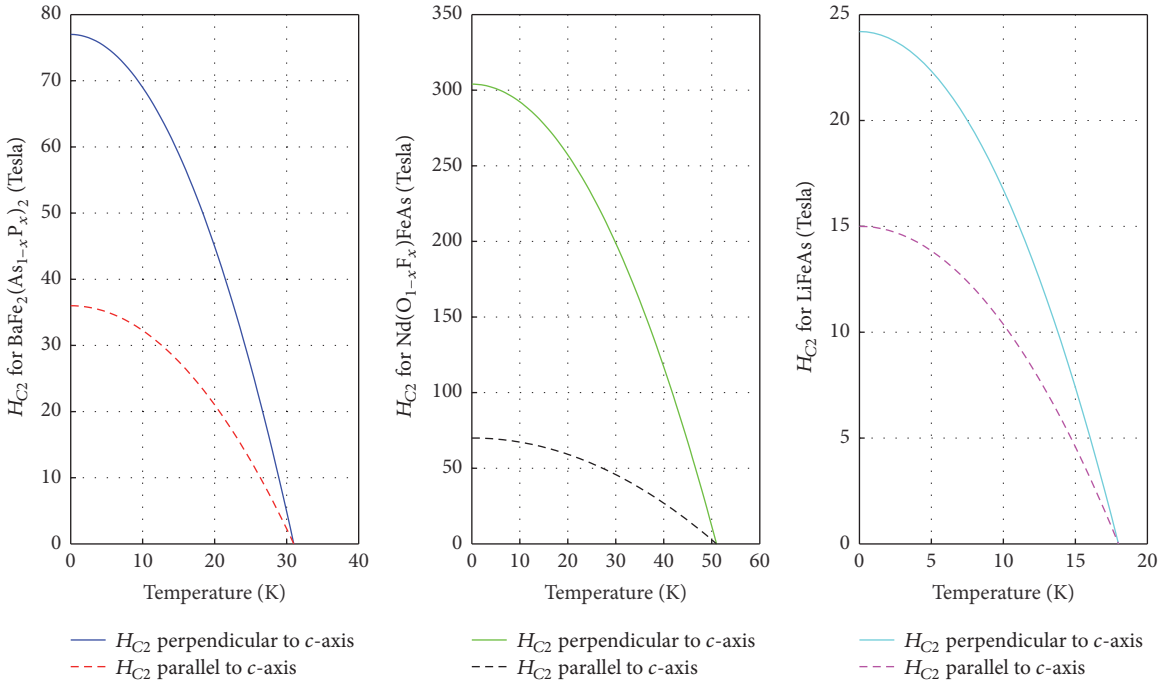

FIGURE 2: The temperature dependence of the upper critical magnetic fields $H_{C2}^{\perp c}$ (solid line) and $H_{C2}^{\parallel c}$ (dashed line) for $BaFe_2(As_{1-x}P_x)_2$, $Nd(O_{1-x}F_x)FeAs$, and LiFeAs.

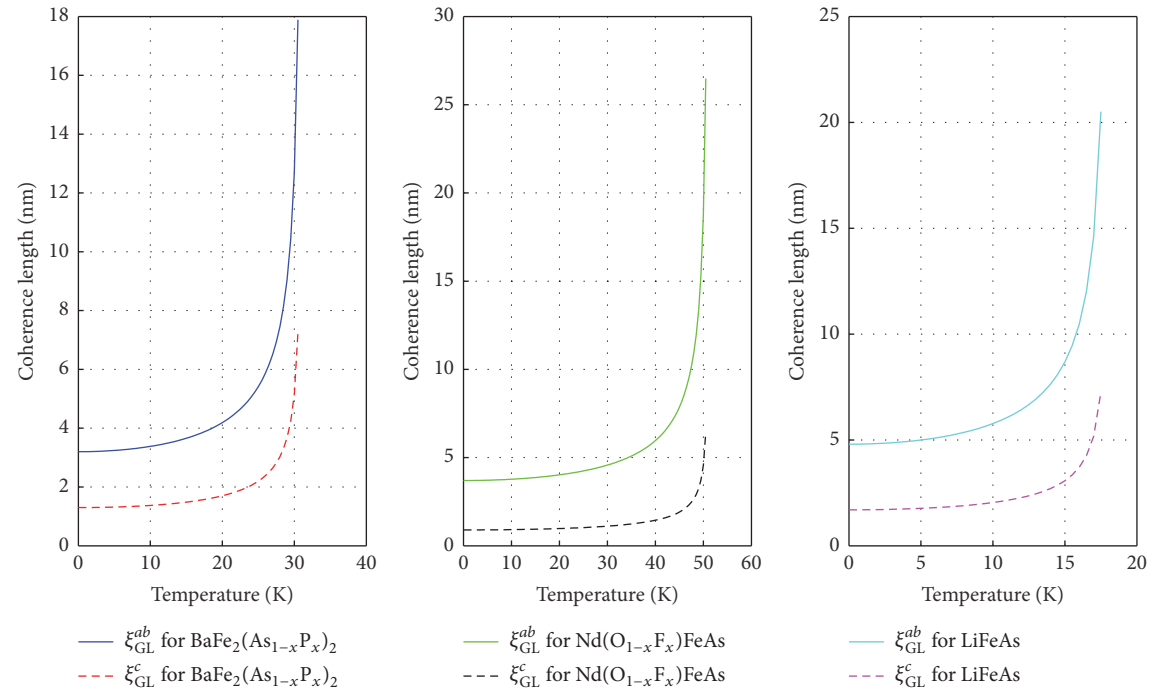

FIGURE 3: The temperature dependence of the GL coherence lengths ξ_{GL}^{ab} (solid line) and ξ_{GL}^{c} (dashed line) for $BaFe_2(As_{1-x}P_x)_2$, $Nd(O_{1-x}F_x)FeAs$, and LiFeAs.

available experimental data, the phase diagrams of ξ_{GL}^{ab} and ξ_{GL}^{c} versus temperature are plotted as shown in Figure 3. As can be seen in Figure 3, the GL coherence length increases with temperature which subsequently diverges at the critical temperature: $\xi_{GL}(T \to T_C) \to \infty$, for $BaFe_2(As_{1-x}P_x)_2$, $Nd(O_{1-x}F_x)FeAs$, and LiFeAs.

Finally, using (45), (46), and (47) and taking the experimental values, we plotted the phase diagrams of λ_{GL}^{ab} and

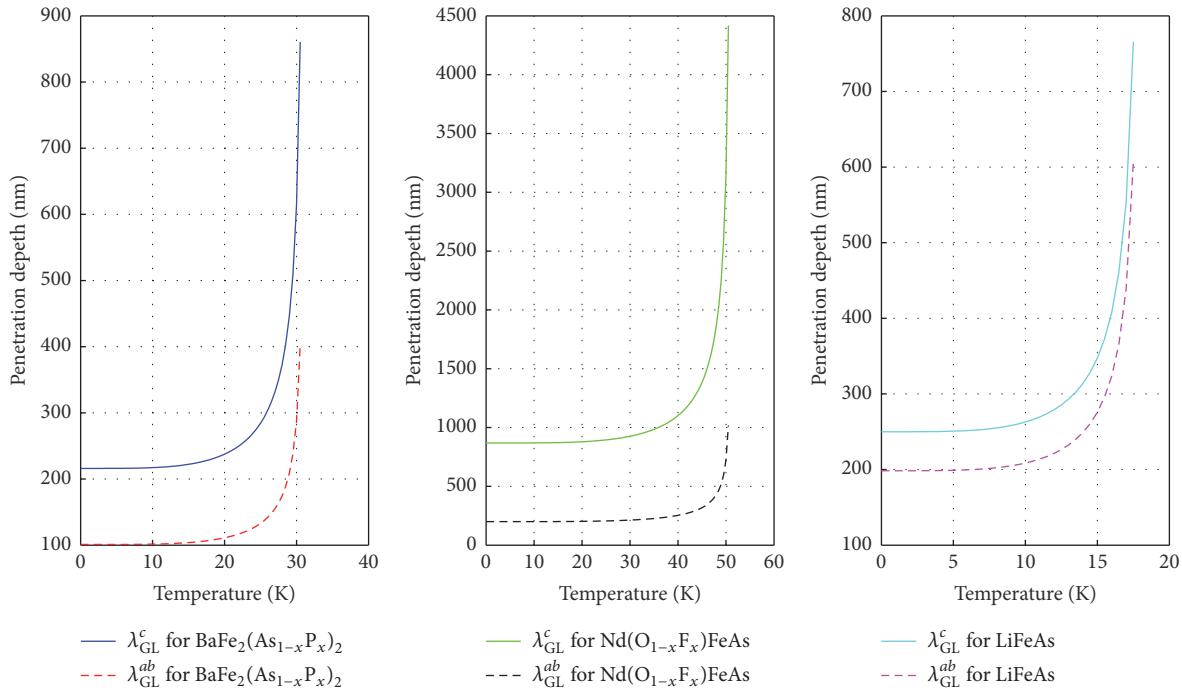

FIGURE 4: The temperature dependence of the GL penetration depths λ^c_{GL} (solid line) and λ^{ab}_{GL} (dashed line) for $BaFe_2(As_{1-x}P_x)_2$, $Nd(O_{1-x}F_x)FeAs$, and LiFeAs.

λ^c_{GL} versus temperature as shown in Figure 4. As can be seen in Figure 4, the GL penetration depth increases with temperature and diverges at the critical temperature, $\lambda_{GL}(T \to T_C) \to \infty$ for $BaFe_2(As_{1-x}P_x)_2$, $Nd(O_{1-x}F_x)FeAs$, and LiFeAs.

4. Conclusion

In this research work, we used two-band GL approach in order to determine the upper critical magnetic field, GL coherence length, and GL penetration depth for the two-band iron based superconductors $BaFe_2(As_{1-x}P_x)_2$, $Nd(O_{1-x}F_x)FeAs$, and LiFeAs. According to the mathematical computations, the coherence length is strongly temperature dependent, so that it can cause temperature dependency and anisotropy nature on the upper critical magnetic field of $BaFe_2(As_{1-x}P_x)_2$, $Nd(O_{1-x}F_x)FeAs$, and LiFeAs. This indicates that the upper critical magnetic field along *ab*-plane, $H^{\perp c}_{C2}$, is quite different from the upper critical magnetic field along *c*-axis, $H^{\parallel c}_{C2}$. We plotted upper critical magnetic field versus temperature phase diagrams and the critical magnetic field decays with increasing temperature as shown in Figure 2. We also plotted GL coherence length and GL penetration depth versus temperature for $BaFe_2(As_{1-x}P_x)_2$, $Nd(O_{1-x}F_x)FeAs$, and LiFeAs and we obtained that the characteristic length increases with temperature and each diverges to infinite at its critical temperature as shown in Figures 3 and 4. Furthermore, we plotted the angular dependence of the upper critical magnetic field for $BaFe_2(As_{1-x}P_x)_2$, $Nd(O_{1-x}F_x)FeAs$, and LiFeAs as shown in Figure 1. Finally, we conclude that the model we used works for $BaFe_2(As_{1-x}P_x)_2$ (122), $Nd(O_{1-x}F_x)FeAs$ (1111), and LiFeAs (111) and the results we obtained are in agreement with experimental findings [4, 19, 22, 27, 29–32].

Competing Interests

The authors declare that there are no competing interests regarding the publication of this paper.

References

[1] Y. Kamihara, T. Watanabe, M. Hirano, and H. Hosono, "Iron-based layered superconductor La[$O_{1-x}F_x$]FeAs ($x = 0.05 - 0.12$) with $T_c = 26$ K," *Journal of the American Chemical Society*, vol. 130, no. 11, pp. 3296–3297, 2008.

[2] H. Takahashi, K. Igawa, K. Arii, Y. Kamihara, M. Hirano, and H. Hosono, "Superconductivity at 43 K in an iron-based layered compound $LaFeAsO_{1-x}F_x$," *Nature*, vol. 453, no. 7193, pp. 376–378, 2008.

[3] A. Nuwal, S. Kakani, and S. L. Kakani, "Generalized multiple gap model for the superconductivity in Fe-As based superconductors," *SOP Transactions on Theoretical Physics*, vol. 1, no. 2, pp. 7–25, 2014.

[4] X. Wang, S. R. Ghorbani, G. Peleckis, and S. Dou, "Very high critical field and superior J_C-field performance in $NdFeAsO_{0.82}F_{0.18}$ with T_C of 51K," *Advanced Materials*, vol. 21, no. 2, pp. 236–239, 2009.

[5] M. Rotter, M. Tegel, and D. Johrendt, "Superconductivity at 38 K in the iron arsenide $(Ba_{1-x}K_x)Fe_2As_2$," *Physical Review Letters*, vol. 101, no. 10, Article ID 107006, 4 pages, 2008.

[6] M. Yamashita, Y. Senshu, T. Shibauchi et al., "Nodal gap structure of superconducting $BaFe_2(As_{1-x}P_x)_2$ from angle-resolved thermal conductivity in a magnetic field," *Physical Review B*, vol. 84, no. 6, Article ID 060507, 4 pages, 2011.

[7] X. C. Wang, Q. Q. Liu, Y. X. Lv et al., "The superconductivity at 18 K in LiFeAs system," *Solid State Communications*, vol. 148, no. 11-12, pp. 538–540, 2008.

[8] F. Wei, F. Chen, K. Sasmal et al., "Temperature dependence of the anisotropy parameter of the LiFeAs upper critical field in the two-band Ginzburg-Landau theory," *Physical Review B*, vol. 81, no. 13, Article ID 134527, 2010.

[9] I. R. Shein and A. I. Ivanovskii, "Electronic properties of novel 6 K superconductor LiFeP in comparison with LiFeAs from first principles calculations," *Solid State Communications*, vol. 150, no. 3-4, pp. 152–156, 2010.

[10] Y. J. Song, J. S. Ghim, B. H. Min, Y. S. Kwon, M. H. Jung, and J.-S. Rhyee, "Growth and characterization of bulk superconductor material," *Applied Physics Letters*, vol. 96, Article ID 212508, 2010.

[11] X. Zhang and Y. Ma, "Development of iron-based superconducting materials for applications," *Chinese Science Bulletin*, vol. 58, no. 11, pp. 986–995, 2013.

[12] A. A. Abrikosov, "On the magnetic properties of superconductors of the second group," *Soviet Physics Journal of Experimental & Theoretical Physics*, vol. 5, pp. 1174–1182, 1957.

[13] V. L. Ginzburg and L. D. Landau, "On the theory of superconductivity," *Soviet Journal of Experimental and Theoretical Physics*, vol. 20, p. 1064, 1950.

[14] J. Bardeen, L. N. Cooper, and J. R. Schrieffer, "Theory of superconductivity," *Physical Review Letters*, vol. 108, pp. 1175–1204, 1957.

[15] O. L. T. de Menezes, "Importance of hybrid pairs in superconductors," *Solid State Communications*, vol. 57, no. 10, pp. 825–828, 1986.

[16] K. Kuroki, S. Onari, R. Arita et al., "Unconventional pairing originating from the disconnected fermi surfaces of superconducting $LaFeAsO_{1-x}F_x$," *Physical Review Letters*, vol. 101, no. 8, Article ID 087004, 4 pages, 2008.

[17] Y. Zhang, L. X. Yang, M. Xu et al., "Nodeless superconducting gap in $A_xFe_2Se_2$ (A = K, Cs) revealed by angle-resolved photoemission spectroscopy," *Nature Materials*, vol. 10, pp. 273–277, 2011.

[18] P. Udomsamuthirun, A. Changjan, C. Kumvongsa, and S. Yoksan, "H_{c2} of anisotropy two-band superconductors by Ginzburg–Landau approach," *Physica C: Superconductivity and Its Applications*, vol. 434, no. 1, pp. 62–66, 2006.

[19] S. V. Chong, S. Hashimoto, and K. Kadowaki, "Upper critical fields and critical current density of BaFe $2(As_{0.68}P_{0.32})_2$ single crystal," *Solid State Communications*, vol. 150, no. 27-28, pp. 1178–1181, 2010.

[20] J. Ketterson and S. Song, *Superconductivity*, Cambridge University Press, New York, NY, USA, 1999.

[21] I. N. Askerzade and B. Tanatar, "Angular dependence of upper critical field in two-band Ginzburg–Landau theory," *Physica C: Superconductivity and Its Applications*, vol. 459, no. 1-2, pp. 56–61, 2007.

[22] J. L. Zhang, L. Jiao, F. F. Balakirev, X. C. Wang, C. Q. Jin, and H. Q. Yuan, "Upper critical field and its anisotropy in LiFeAs," *Physical Review B*, vol. 83, no. 17, Article ID 174506, 2011.

[23] A. Changjan and P. Udomsamuthirun, "Critical magnetic field ratio of anisotropic magnetic superconductors," *Physica C: Superconductivity and Its Applications*, vol. 471, no. 1-2, pp. 23–25, 2011.

[24] U. Welp, R. Xie, A. E. Koshelev et al., "Calorimetric determination of the upper critical fields and anisotropy of $NdFeAsO_{1-x}F_x$ single crystals," *Physical Review B*, vol. 78, no. 14, Article ID 140510, 4 pages, 2008.

[25] C. J. Gorter and H. B. G. Casimir, "On supraconductivity I," *Physica*, vol. 1, no. 1–6, pp. 306–320, 1934.

[26] C. Chaparro, L. Fang, H. Claus et al., "Doping dependence of the specific heat of single crystal $BaFe_2(As_{1-x}P_x)_2$," https://arxiv.org/abs/1110.3075.

[27] Y. Jang Song, J. S. Ghim, J. H. Yoon et al., "Small anisotropy of the lower critical field and the $s_{\pm}$-wave two-gap feature in single-crystal LiFeAs," *EPL*, vol. 94, no. 5, Article ID 57008, 2011.

[28] S. Weyeneth, R. Puzniak, N. D. Zhigadlo et al., "Evidence for two distinct anisotropies in the oxypnictide superconductors $SmFeAsO_{0.8}F_{0.2}$ and $NdFeAsO_{0.8}F_{0.2}$," *Journal of Superconductivity and Novel Magnetism*, vol. 22, no. 4, pp. 347–351, 2009.

[29] A. Ramos-Álvarez, J. Mosqueira, F. Vidal et al., "Superconducting fluctuations in isovalently substituted $BaFe_2(As_{1-x}P_x)_2$: possible observation of multiband effects," *Physical Review B—Condensed Matter and Materials Physics*, vol. 92, no. 9, Article ID 094508, 2015.

[30] Y. Jia, P. Cheng, L. Fang et al., "Critical Fields and Anisotropy of $NdFeAsO_{0.82}F_{0.18}$ single crystals," *Applied Physics Letters*, vol. 93, no. 3, Article ID 032503, 2008.

[31] C. K. H. Borg, X. Zhou, C. Eckberg et al., "Strong anisotropy in nearly ideal tetrahedral superconducting FeS single crystals," *Physical Review B*, vol. 93, no. 9, Article ID 094522, 10 pages, 2016.

[32] R. Prozorov, M. A. Tanatar, R. T. Gordon et al., "Anisotropic London penetration depth and superfluid density in single crystals of iron-based pnictide superconductors," *Physica C: Superconductivity and Its Applications*, vol. 469, no. 9–12, pp. 582–589, 2009.